JOURNAL OF MATERIALS SCIENCE 22 (1987) 219–222

The structure and optical response of a nickel black selective coating

S. ABIS
Aluminia S.p.A., Istituto Sperimentale Metalli Leggeri, Via Fauser 4, 28100 Novara, Italy

A simple model based on a suspension of metallic nickel particles in a semiconducting matrix, is proposed to explain some optical features of a selective nickel black coating developed for solar energy exploitation. The optical response in the visible and near infrared range is calculated by means of effective medium theories, and the results are discussed in relation to experimental data.

1. Introduction

This paper describes experimental and theoretical work on the optical response of an electrodeposited selective nickel black coating developed for solar energy exploitation by photothermal conversion. This kind of coating was first described by Tabor [1] and then widely investigated by other researchers [2–8]. It can be obtained by chemical conversion of a zinc-coated substrate, or by electrodeposition on a nickel or zinc substrate from baths containing nickel and zinc sulphates.

The main features of electrodeposited nickel black are the low current density required for deposition and fewer problems of pollution compared to other well known coatings such as chromium black. It nevertheless exhibits a poor resistance in a humid environment and rapidly decomposes over 200° C in air. The first problem can be solved by an appropriate passivation process (as an example, a chromium oxide passivation can be considered [9]), but the second problem limits the use of the coating to low temperature environments.

The structure of this film seems to be a fine suspension of metallic particles embedded in a semiconducting bulk, somewhat like nickel-pigmented Al_2O_3 [10] or chromium black [11]. Some features of nickel black are described here and discussed with the aid of a numerical model. In particular a two-layer structure on a substrate is proposed to explain the optical response of the coating in the visible and near infrared range.

2. Materials and methods

2.1. Sample Preparation

The coating has been developed for use in solar panels employing Aluminium AA 6060 alloy extruded bars. Specimens used in this work have therefore been prepared following the usual industrial process: a zinc film was deposited on to flat 100 mm × 100 mm × 1 mm 6060 Al alloy sheets obtained from rolling extruded strips. They were then electroplated with a nickel-Watt film and then coated with a nickel black film; the whole process is described in Table I.

2.2. SEM EDS examinations

Scanning electron microscopy (SEM) has been used to observe the morphological characteristics of the film. The nickel black coating was intentionally fractured by excessive bending and then an extremely thin layer of gold was sputtered on to the film to make it conductive.

SEM observation does not give evidence for any particular structure, as can be seen in Fig. 1; in particular the fracture surface indicates a compact layer without columnar structures as in [10] or more complicate morphologies as in [11].

The thickness of the film has been estimated as 0.6 μm, and it was almost constant in different parts of the specimen. A microprobe energy dispersion (EDS) analysis performed on the surface of the sample revealed energy peaks for nickel, zinc and sulphur (oxygen was out of the range of the instrument) as shown in Fig. 2.

2.3. Reflectance measurements

Reflectance measurements have been performed on discs of 55 mm diameter obtained from coated samples. The hemispherical reflectivity has been measured in the range 0.36 to 2.7 μm of wavelength by using a Perkin Elmer DK2 with MgO as reference. The specular component of reflectivity was monitored in the near infrared (2.5 to 15 μm) by a Perkin Elmer IR21 using an aluminium mirror as reference: in this range the diffuse component can be considered negligible. This can be tested by comparing results in the overlap range (2.5 to 2.7 μm), Fig. 3 shows a typical reflectivity curve of the nickel black.

2.4. Auger examinations

Auger profiling data have been obtained for various components of the coated film: results are shown in Fig. 4. Components of the coating are nickel, zinc, sulphur and oxygen. The profile of carbon has also been determined to test the contamination characteristics of the outer surface. An X-ray photoelectron spectroscopy (XPS) analysis performed at various depths revealed the presence of nickel in the metallic

0022–2461/87 $03.00 + .12 © *1987 Chapman and Hall Ltd.*

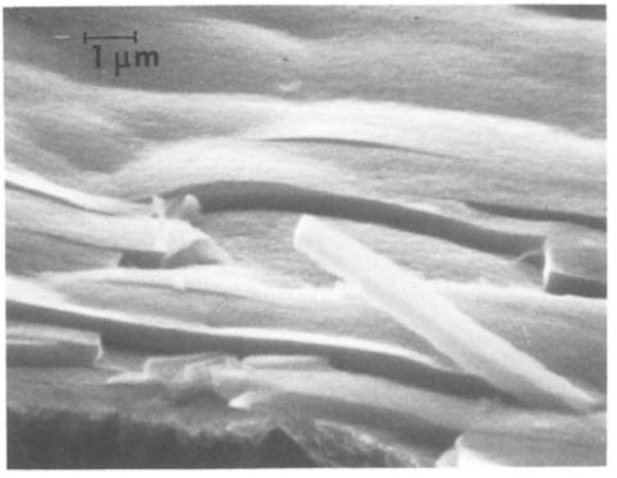

Figure 1 SEM image of the nickel black coating. It has been broken by excessive bending, and then an extremely thin layer of gold has been sputtered on to the film to make it conductive.

state (24 at %) and zinc as a mixture of ZnS and ZnO; a higher content of ZnO was detected in the outer part of the film and a lower one in the bulk; the analysis did not show zinc in the metallic state.

The profile of nickel is not constant throughout the film thickness; in particular an XPS analysis performed on the surface did not reveal the presence of nickel, while after 2 min of ionic sputtering, a high content of metallic nickel appeared.

3. Theoretical model

From the experimental evidence, we can try to formulate a model of the film structure based on a fine suspension of metallic nickel particles embedded in a ZnO/ZnS matrix. The consistency of the model can be tested, with the aid of effective medium theories, by calculating the reflectivity of the film and comparing calculations with experimental data.

It is well known that selective coatings deposited on to transition metal substrates act in the visible range only by lowering the reflectivity, while in the infrared range the optical response is mainly due to the metallic substrate. Therefore attention has to be paid, mainly, to the wavelength range 0.36 to 2.5 μm where the structure of the film is of prime importance, while for larger wavelength, λ, the reflectivity of nickel black tends to overlap the response of the nickel substrate.

TABLE I Preparation parameters of the nickel black samples used in this work

Material	Thickness (mm)	Reference
Substrate: Al–Mg–Si alloy 6060	1	–
Zn undercoat	0.001	[24]
Ni-Watt	0.020	[24]
Nickel black	0.006	[8]

For a single homogeneous layer of film on a substrate the reflectivity function, $R(\lambda)$, can be obtained as [12]:

$$R(\lambda) = \left| \frac{\cos\chi + iN\sin\chi + N_s[-(i\sin\chi)/N - \cos\chi]}{\cos\chi - iN\sin\chi + N_s[-(i\sin\chi)/N + \cos\chi]} \right|^2 \quad (1)$$

with $\chi = 2\pi NT\lambda^{-1}$; N and N_s are the refractive indices of the film and the substrate, respectively, and T the thickness of the coating.

The refractive index $N = \varepsilon^{1/2}$ (ε is the dielectric permeability) of the film can be calculated by using both the theory of Maxwell-Garnett [13] or Bruggeman [14]. According to Maxwell-Garnell, the value $\bar{\varepsilon}^{MG}$ for the effective permeability of an inhomogeneous material with spherical particles of permeability ε embedded in a medium with permeability ε_m, is:

$$\bar{\varepsilon}^{MG} = \varepsilon_m \left[1 + \tfrac{2}{3}F\frac{\varepsilon - \varepsilon_m}{\varepsilon_m + \frac{1}{3}(\varepsilon - \varepsilon_m)} \right] \times \left[1 - \tfrac{1}{3}F\frac{\varepsilon - \varepsilon_m}{\varepsilon + \frac{1}{3}(\varepsilon - \varepsilon_m)} \right]^{-1} \quad (2)$$

The Bruggeman theory states that, in the same conditions,

$$\bar{\varepsilon}^{Br} = \varepsilon_m \left(1 - F + \tfrac{1}{3}F\frac{\varepsilon - \bar{\varepsilon}^{Br}}{\bar{\varepsilon}^{Br} + \frac{1}{2}} \right) \quad (3)$$

F is the filling factor in both cases. Equations 2 and 3 can be generalized to comprise several shapes of embedded particles as well as more complicated shapes and size distributions [15–19]. Furthermore,

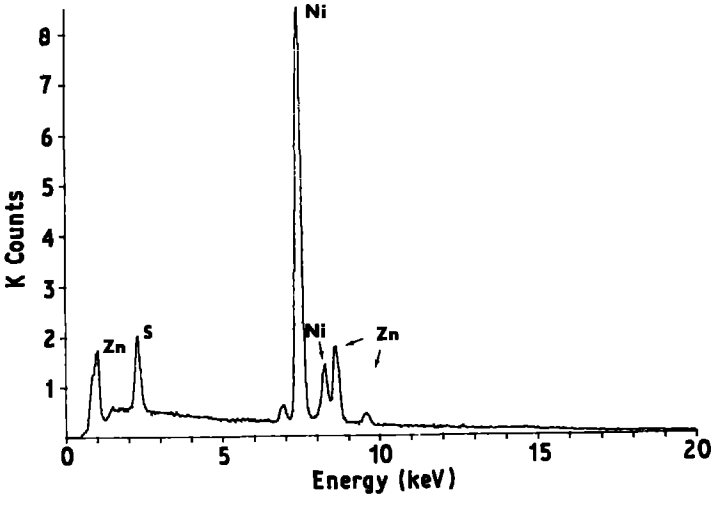

Figure 2 EDS analysis carried out on the sample of Fig. 1. The film contains zinc, nickel and sulphur (oxygen is out of the range of detection). The Ni($K\alpha$) peak is probably influenced by the substrate.

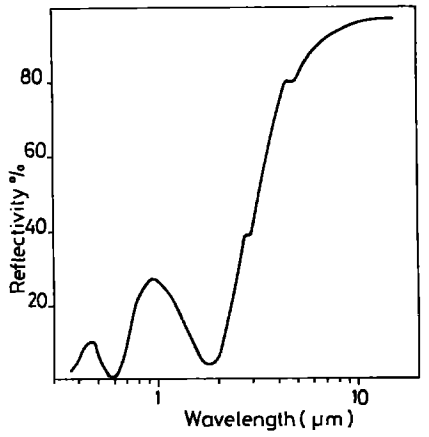

Figure 3 Typical reflectivity curve. In the range 2.5 to 3 μm the curves obtained by hemispherical and specular measurements have been averaged to give the curve below.

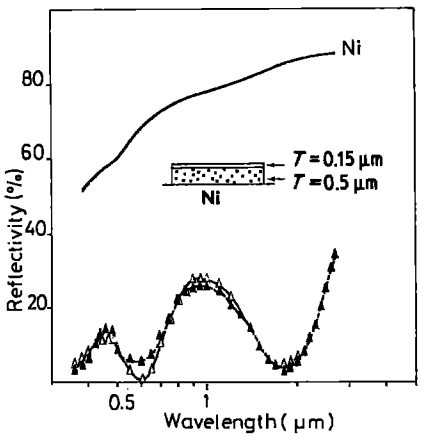

Figure 5 Experimental (△) and theoretical (▲) curves obtained by using a two-layer model. The curves are compared to the reflectivity of metallic nickel according to Johnson and Christy [21]. A filling factor $F = 0.015$ has been considered for the outer layer.

Equation 1 can be obviously extended to calculate the reflectance response for multilayer systems.

Starting from experimental results, the most simple model to try is a two-layer model based on a suspension of metallic nickel spheres embedded in a ZnS/ZnO matrix. The two layers in the film are on a nickel substrate. The particular peaked $R(\lambda)$ curve and Auger profiles suggest a model where a thinner layer of ZnO ($= 0.15\,\mu$m thick) characterized by a low filling factor, F, is deposited on to a thicker one ($= 0.5\,\mu$) ZnS layer with a filling factor corresponding to a nickel content of 24 at %. For these values of nickel content, results obtained by using the Bruggeman or the Maxwell-Garnett theory tend to overlap. By using the Bruggeman theory, and data tabulated by Bond [20] for physical properties of ZnS and ZnO, and by Johnson and Christy [21] for metallic nickel, such a model compares well, with reasonable accuracy, to the experimental $R(\lambda)$ curve.

In Fig. 5 results obtained from calculations are compared with the experimental $R(\lambda)$ curve in the range 0.45 to 2.5 μm; a r.m.s. roughness $\sigma = 0.03$ has been used as suggested by Davies [22] to take into account the few small-scale thickness variations of the outer layer.

A value of absorptivity $\alpha = 0.85$, can be obtained by integration of the $R(\lambda)$ curve in the range of wavelength 0.45 to 2.5 μm following the formula:

$$\alpha = 1 - \frac{\int_{\lambda_1}^{\lambda_2} R(\lambda)\,\mathrm{d}\lambda}{(\lambda_2 - \lambda_1)} \qquad (4)$$

in good agreement with the experimental value of $\alpha = 0.87$ obtained in the same range of wavelength.

As pointed out in a previous paper [23] a severe deterioration occurs following exposure in a humid environment, causing a decrease in the optical performance of the selective film. This is probably due to hydration of the thinner external layer. Fig. 6 shows the features of the $R(\lambda)$ curves obtained on samples exposed in humid environment for increasing times (72 and 144 h at 40° C, 98% r.h.) The peaked structure (in particular the minimum between 1.5 and 2 μm) tends to vanish, and an Auger profile performed on a sample after 24 h exposure shows a severe deterioration of the outer layer (Fig. 7).

The optical effect can be numerically simulated by adopting a two-layer model where, with respect to the previous one, the total thickness remains unchanged, but the outer film is thicker. Moreover, due to the hydration effect, a lowering of the mean refractive index can be expected. The last picture (Fig. 8) shows the results of calculations performed on a model

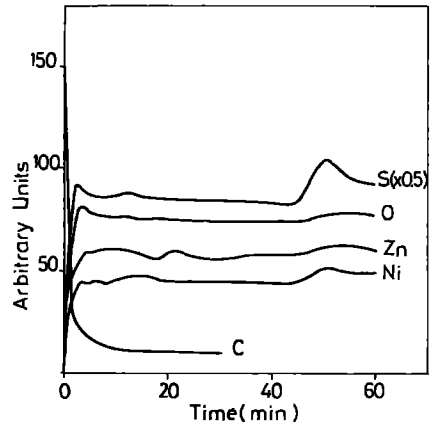

Figure 4 Auger depth profile of the components of the film. The time is the sputter time.

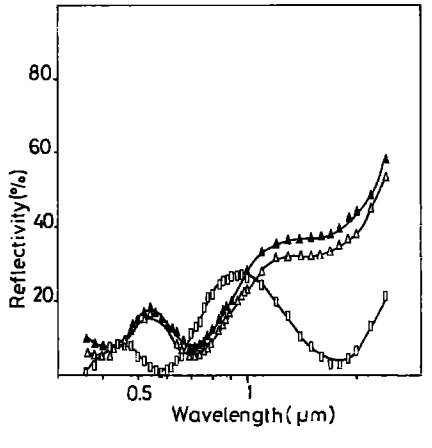

Figure 6 Effect of exposure in a humid environment (40° C; 98% r.h.) on the $R(\lambda)$ curve: (a) (□) as-prepared; (b) (△) after 72 h exposure; (c) (▲) after 144 h.

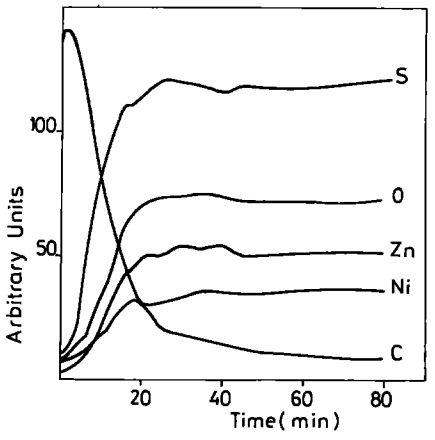

Figure 7 Auger depth profile performed on a sample after 24 h of exposure in a humid environment.

where the changes in the optical characteristics are simulated by adopting proper values for the various parameters. As can be seen, the trend of the $R(\lambda)$ curves is in qualitative agreement with the experimental results of the previous figure.

4. Conclusion

Some features of the optical response of a selective nickel black coating can be explained, on the basis of a two-layer model on a substrate, by considering the film as a fine suspension of metallic nickel particles embedded in a semicondicting ZnS/ZnO matrix.

Calculations of the optical response on the basis of this hypothesis compare well with the experimental results.

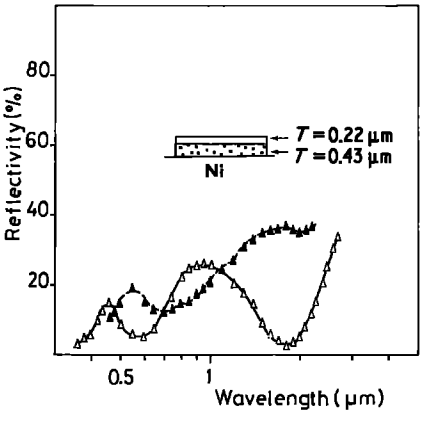

Figure 8 Results of calculations carried out on a model simulating the degradation of the optical characteristics by exposure in a humid environment. For the outer layer a refractive index of 1.8 has been used, irrespective of wavelength, for the bulk material. The filling factors remain unchanged. (a) (△) As in Fig. 5; (b) (▲) after simulated exposure.

Obviously the model presented here could be refined, for example by considering non-spherical particles, but it would probably be redundant, because more precise experimental data are not available at present. The most important conclusion is, therefore, that metallic particles embedded in a semiconducting matrix play an important role in determining the selectivity characteristics of the film.

The structure of this coating seems to be similar to that of other well-known selective films such as chromium black or nickel-pigmented Al_2O_3.

References

1. H. TABOR, "Transactions of the Conference on the use of Solar Energy", Vol 2, Tucson, Arizona (1956) p. 14.
2. H. Y. B. MAR and J. H. LIN, "Optical Coatings for Flat Plate Solar Collectors", Final Report ERDA, Division of Solar Energy COO/2625/75/1 (1975).
3. K. J. CATHRO, *Sol. Energy Mater.* **5** (1981) 317.
4. P. K. GOGNA and K. L. CHOPRA, *Sol. Energy* **23** (1979) 405.
5. S. N. KUMAR, L. K. MALHOTRA and K. L. CHOPRA, *Sol. Energy Mater.* **3** (1980) 519.
6. A. EGGERS-LUCRA, "Flat Plate Solar Collectors and Their Application to Dwelling", Report for the Commission of the European Communities, Contract no. 207-75-9ECJ (1976) p. 19.
7. J. H. LIN and R. E. PETERSON, "Proceedings of the Meeting of the Society for Photo-Optical Instrumentation Engineers", San Diego, California Vol. 85 (1976) p. 62.
8. B. A. SHENOI and K. S. INDIRA, *Met. Finish.* **61** (1963) 65.
9. R. E. VAN DE LEEST, B. VAN DER WERT and G. KRIJL, *Sol. Energy* **26** (1981) 551.
10. A. ANDERSON, O. HLINDERI and C. G. GRANQVIST, *J. Appl. Phys.* **51** (1980) 754.
11. G. ZAJAC, G. B. SMITH and A. IGMATIE, *ibid.* **51** (1980) 5544.
12. A. VASICEK, "Optics of Thin Films" (North Holland, Amsterdam, 1960).
13. J. C. H. GARNETT, *Phil. Trans. R. Soc. Lond.* **203** (1904) 385.
14. D. A. G. BRUGGEMAN *Ann. Phys. (Leipzig)* **24** (1935) 636.
15. C. G. GRANQVIST and O. HUNDERI, *Appl. Phys. Lett.* **32** (1978) 798.
16. *Idem, Phys. Rev. B.* **16** (1977) 3513.
17. *Idem, Z. Phys. B* **30** (1978) 47.
18. *Idem, Phys. Rev. B* **18** (1978) 1554.
19. *Idem, J. Appl. Phys.* **50** (1979) 1058.
20. W. L. BOND, *J. Appl. Phys.* **36** (1965) 1974.
21. P. B. JOHNSON and R. W. CHRISTY, *Phys. Rev. B.* **9** (1974) 5056.
22. H. DAVIES, *Proc. IEEE* **101** (1954) 209.
23. S. ABIS M. L. LORENZETTI, *J. Mater. Sci. Lett.* **4** (1985) 1102.
24. E. BERTORELLE, "Trattato di galvanotecnica", Vol. II (Hoepli, Milano, Italy, 1978) p. 498.

Received 30 December 1985
and accepted 6 May 1986